GPS Solut (2013) 17:29–39
DOI 10.1007/s10291-012-0258-8

ORIGINAL ARTICLE

GPS-PWV estimation and validation with radiosonde data and numerical weather prediction model in Antarctica

G. Esteban Vázquez B · Dorota A. Grejner-Brzezinska

Received: 20 January 2011 / Accepted: 7 February 2012 / Published online: 3 March 2012

Abstract Three permanent GPS tracking stations in the trans Antarctic mountain deformation (TAMDEF) network were used to estimate precipitable water vapor (PWV) using measurement series covering the period of 2002–2005. TAMDEF is a National Science Foundation funded joint project between The Ohio State University and the United States Geological Survey. The TAMDEF sites with the longest GPS data spans considered in this research are Franklin Island East (FIE0), the International GNSS Service site McMurdo (MCM4), and Cape Roberts (ROB1). For the experiment, PWV was extracted from the ionosphere-free double-difference carrier phase observations, processed using the adjustment of GPS ephemerides (PAGES) software. The GPS data were processed with a 30 s sampling rate, 15-degree cutoff angle, and precise GPS orbits disseminated by IGS. The time-varying part of the zenith wet delay is estimated using the Marini mapping function, while the constant part is evaluated using the corresponding Marini tropospheric model. Previous studies using TAMDEF data for PWV estimation show that the Marini mapping function performs the best among the models offered by PAGES. The data reduction to compute the zenith wet delay follows the step piecewise linear strategy, which is subsequently transformed to PWV. The resulting GPS-based PWV is compared to the radiosonde observations and to values obtained from the Antarctic mesoscale prediction system (AMPS). This comparison revealed a consistent bias of 1.7 mm between the GPS solution and the radiosonde and AMPS reference values.

Keywords GPS · PWV · Radiosonde · AMPS · TAMDEF · Antarctica

G. E. Vázquez B (✉)
Earth Science School, The Autonomous University of Sinaloa, 1841 Océano Pacifico, Col. Nuevo Culiacán, C.P.80170 Culiacán, Sinaloa, Mexico
e-mail: gvazquez@uas.uasnet.mx

D. A. Grejner-Brzezinska
Satellite Positioning and Inertial Navigation (SPIN) Laboratory, The Ohio State University, Columbus, OH, USA

Introduction

The TAMDEF network (Vázquez 2009) is a GPS array deployed on bedrock, consisting of 25 campaign sites, six quasi-continuous sites, and two continuous sites located in the Trans Antarctic Mountains of the southern Victoria Land and on the islands in the adjacent Ross Sea (Fig. 1). TAMDEF is the OSU and USGS joint project sponsored by the NSF, initiated in 1996 with the primary objective to measure vertical and horizontal crustal deformation. Three TAMDEF sites, FIE0, MCM4, and ROB1 with longest GPS data spans, were used in this experiment to estimate GPS-PWV values. To determine the quality of the GPS-derived PWV, the estimates for site MCM4 are compared to radiosonde measurements of PWV and subsequently compared to the values extracted from the AMPS (Powers et al. 2003). AMPS is a mesoscale numerical weather prediction model that has been tuned to work in the Antarctic environment and currently provides guidance for operations-based forecasts for the United States Antarctic Program (USAP). It was demonstrated by Bromwich et al. (2005) and Fogt and Bromwich (2008) that AMPS performance in moisture and cloud variability prediction is not satisfactory. Thus, comparing the AMPS forecasts with the GPS-PWV and radiosonde estimates should allow for a better understanding of the model prediction of moist processes. In the future, it is anticipated that assimilated

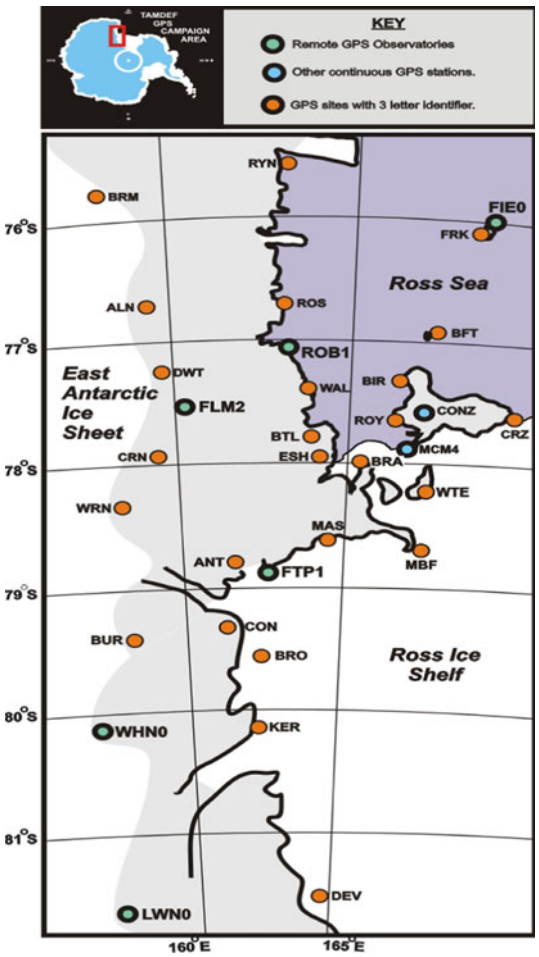

Fig. 1 TAMDEF network, Victoria Land, Antarctica

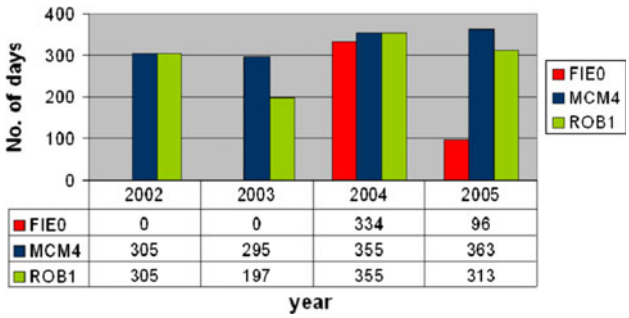

	2002	2003	2004	2005
FIE0	0	0	334	96
MCM4	305	295	355	363
ROB1	305	197	355	313

Fig. 2 GPS data spans for TAMDEF sites

Fig. 3 Franklin Island East, FIE0 site

Fig. 4 MCM4 site at McMurdo

GPS-PWV estimates will aid in improving the moisture prediction in AMPS, thereby leading to increased forecast accuracy, which is essential for efficiency and safety of all USAP operations.

Test description and data processing

Three TAMDEF sites, FIE0, MCM4, and ROB1, situated at the Trans Antarctic Mountains of the southern Victoria Land and on the islands in the adjacent Ross Sea in Antarctica with long data spans (Fig. 2) were used in this experiment to estimate PWV values from GPS.

The surrounding area for the GPS sites can be seen in Figs. 3, 4, 5. Both FIE0 and ROB1 stations are located at the Ross Ice Shelf; the first site is in a marine environment with very difficult access, while the second site is more accessible but with the presence of some rocks. MCM4 is located at base McMurdo with a dome covering the antenna site. It is very important to point out that there was no antenna replacement since the installation of this site. Also, note that seasonal moisture condensation can be seen inside the radome.

The GPS hardware characteristics, such as the receiver type, antenna make and model, and the IGS designator, used at each site are presented in Table 1. Note that the antenna for the MCM4 site has not been calibrated and this might have an impact on the final PWV estimates for this site.

Dual-frequency geodetic-grade GPS receivers were used for the GPS data collection in static mode at the three

Antarctic sites. GPS data were downloaded, converted to RINEX format, and the quality and integrity of the RINEX files were checked with the Test of Quality Check (TEQC) free software, provided by University NAVstar Consortium (UNAVCO). Then, the NGS PAGES software (Eckl et al. 2001; Mader et al. 1995; Schenewerk et al. 2001) was used to process the GPS data using the ionosphere-free, double-difference carrier phase observations given by

$$\Phi^{km}_{ij,Lm,n} = \rho^{kl}_{ij} + T^{kl}_{ij} + \alpha_{L1}\lambda_{L1}N_{L1} + \alpha_{L2}\lambda_{L2}N_{L2} + \alpha_{L1}\varepsilon^{kl}_{ij,L1} + \alpha_{L2}\varepsilon^{kl}_{ij,L2} \quad (1)$$

with $\alpha_{L_1} = \frac{f^2_{L1}}{f^2_{L_1} - f^2_{L_2}}$ and $\alpha_{L_2} = -\frac{f^2_{L2}}{f^2_{L_1} - f^2_{L_2}}$ where subscripts i, j denote receivers, superscripts k, l denote satellites, ρ^{kl}_{ij} is the geometric distance between satellites and receivers, $L_{m,n}$ denotes frequencies, m for L_1 and n for L_2, respectively, T^{kl}_{ij} is the tropospheric refraction term, $\lambda_{L_1} \approx 19$ cm and $\lambda_{L_2} \approx 24$ cm are the wavelengths on L_1 and L_2 carrier, N_{L1} and N_{L2} are the ambiguities, $\varepsilon^{kl}_{ij,L_1}$ and $\varepsilon^{kl}_{ij,L_2}$ is the measurement noise for L_1 and L_2, respectively. Other specifications for the processing were: elevation mask of 15 degrees, data sampling interval of 30 s, and use of precise ephemeris. Also, the carrier phase ambiguity parameters were fixed at the rate of 97–100% in all solutions.

At first instance, for the GPS data processing scheme with PAGES software, position of the MCM4 (known) site was fixed with respect to International Terrestrial Reference Frame (ITRF00) at reference epoch 2005.5, and coordinates of FIE0 and ROB1 were resolved. Next, the a priori coordinates for the three TAMDEF sites were very tightly constrained to their previously estimated values; that is, practically fixed to a previous network solution in order to compute the zenith wet delay (ZWD) that is later transformed to PWV using the Bevis et al. (1992) approach. In all, eight values per station for the atmospheric ZWD were estimated in a 24-h batch solution, resulting in PWV estimates every 3 h for the entire process.

Fig. 5 The ROB1 site at Cape Roberts

Surface temperature and pressure for the test sites

According to Bevis et al. (1992), converting ZWD to PWV requires temperature profiles, which are obtained from surface values. Also, surface pressure is needed to evaluate the dry tropospheric delay, which is removed from the total zenith delay (TZD) to derive ZWD. The a priori hourly average estimates of surface temperature and surface pressure were determined from the National Centers for Environmental Prediction/National Center for Atmospheric Research (NCEP/NCAR) reanalyzes based on Bromwich and Fogt (2004). Temperature values at 2 m above the ground were estimated every hour and they are shown in Fig. 6, while surface pressure values for the years 2002–2005 are shown in Fig. 7.

Zenith wet delay (ZWD) estimation

The atmospheric layer between the surface of the earth and the ionosphere is called the neutral atmosphere, the lowest portion of which is the troposphere. The tropospheric delay caused by the neutral atmosphere consists of two components: the *hydrostatic* or *dry* component, which is dependent on the dry air gases in the atmosphere and accounts for approximately 90% of the delay, and the *wet* component that depends upon the moisture contents of the atmosphere and contains significant levels of water vapor; it accounts for the remaining effect of the delay (Emardson et al. 2003; Dodson et al. 1996). In terms of the modeling/estimation of the tropospheric corrections, the wet component is indeed more difficult to accomplish in comparison with the dry component.

In order to account for tropospheric corrections, Schenewerk (2004) recommends that for baselines similar as

Table 1 Description of the GPS hardware

Site	Receiver type	Antenna make and model	IGS designator
FIE0	TPS HE_GGD	Thales and astech D/M + radome	ASH701945B_M SCIS
MCM4	AOASNR12-ACT	Allen osborne dorne margolin	AOAD/M_T JPLA
ROB1	TPS HE_GD	Ashtech choke ring + radome	ASH700936D_M SCIS

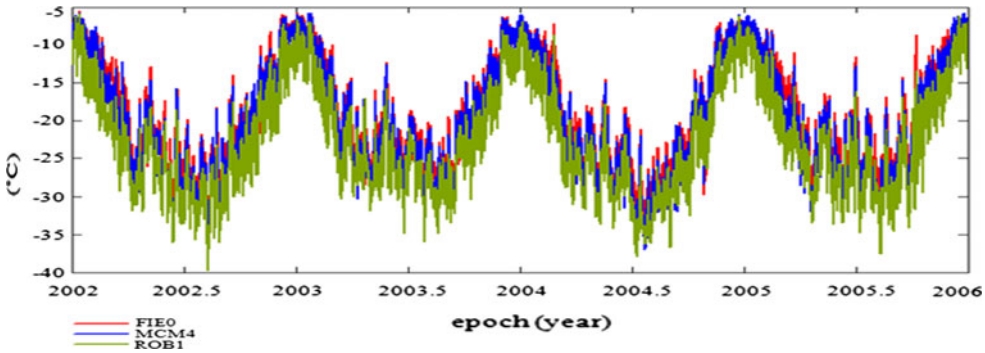

Fig. 6 Surface temperature for FIE0, MCM4, and ROB1

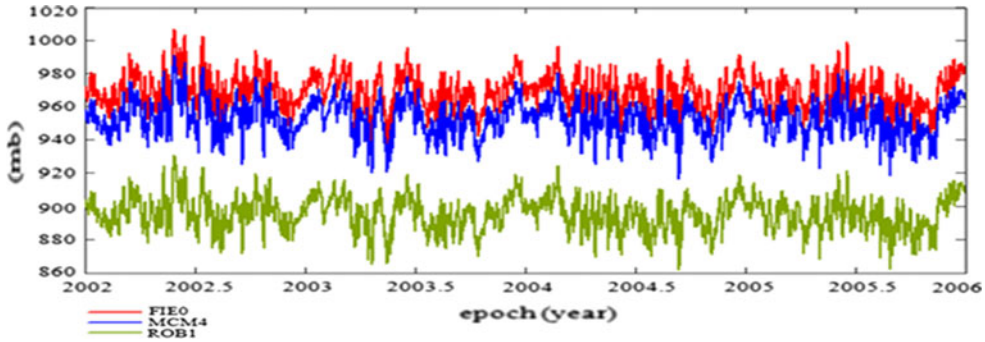

Fig. 7 Surface pressure for FIE0, MCM4, and ROB1

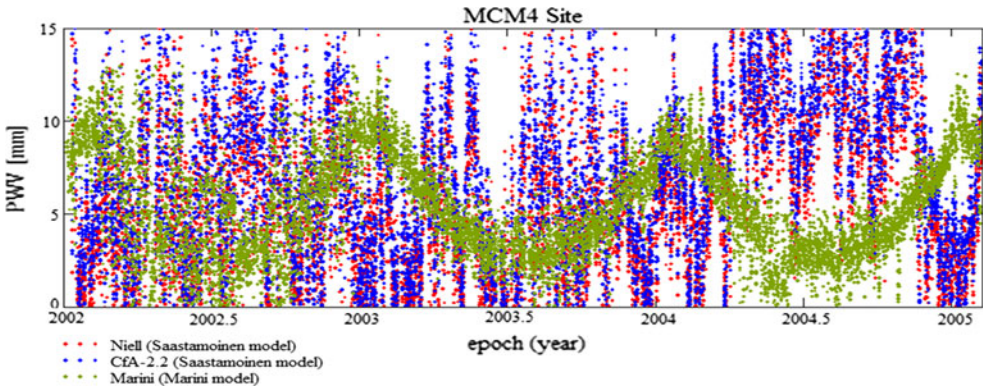

Fig. 8 Preliminary results for GPS-PWV for MCM4 using the Niell, CfA-2.2, and Marini mapping functions with their corresponding Saastamoinen and Marini tropospheric models (Vázquez and Brzezinska 2005)

those in TAMDEF network with length larger than 50 km, absolute tropospheric corrections need to be estimated based on the appropriate selection of the corresponding tropospheric models coded inside PAGES software. In general, these models require parameters, such as temperature, pressure, and relative humidity that usually represent the mean values of an entire column of air, but typically they are replaced by surface meteorological values instead. Thus, the Marini (1972) model with its corresponding Marini mapping function was selected in PAGES to properly model the tropospheric effects because preliminary studies described in Vázquez and Brzezinska (2005) on the use of TAMDEF data for PWV estimation show that the Marini mapping function performs best among the models offered by PAGES. Evidence of this issue is presented in Fig. 8 where GPS-PWV time series for 2000–2005 were computed for MCM4 station by three different mapping functions with their corresponding tropospheric model. The Marini mapping function with the Marini model performs with the highest skill on the TAMDEF data as indicated by the mean and the standard deviation values, 30–40% less as compared with the other mapping functions. Hence, hereinafter, the GPS-PWV results presented next were generated using the Marini mapping function with the Marini model.

The zenith dry part of the troposphere Z_{dry} was modeled and then removed, while the corrections for the zenith wet delay Z_{wet} were only estimated based on the step piecewise

linear strategy at a 3-h interval that considers the time-dependent behavior of the neutral atmospheric delay (Lancaster and Salkauskas 1986). In addition, according to Marshall et al. (2001), considering that GPS signals pass through more of the neutral atmosphere as the satellite elevation angle E decreases, the mapping function

$$T(E) = m_{\text{dry}}(E) \cdot Z_{\text{dry}} + m_{\text{wet}}(E) \cdot Z_{\text{wet}} \tag{2}$$

is used to obtain the slant delay $T(E)$ as function of the satellite's elevation angle. The factor $m_{\text{dry}}(E)$ is the mapping function associated with Z_{dry}, and $m_{\text{wet}}(E)$ is that of the Z_{wet}.

Furthermore, evaluation of Eq. 2 requires external surface temperature and pressure obtained via external meteorological files. Considering that Z_{wet} experiences rapid temporal and spatial variation relative to Z_{dry}, the PAGES software allows that the unknown parameters lie within the ionosphere-free DD carrier phase observation equation given by Eq. 1. For this reason, and following the discussion provided by Marshall et al. (2001), the parameters associated with the ground stations i and j, denoted by $\delta Z_{\text{wet},i}$ and $\delta Z_{\text{wet},j}$, appear in the one-way neutral atmospheric delays, namely

$$T_{ij}^{kl} = \left[T(E_i^k) - T(E_i^l)\right] - \left[T(E_j^k) - T(E_j^l)\right] \tag{3}$$

By using Eq. 2, any of the four delays, for example, $T(E_i^k)$, can be linearized as follows:

$$T(E_i^k) = m_{\text{dry}}(E_i^k) Z_{\text{dry},i} + m_{\text{wet}}(E_i^k) Z_{\text{wet},i} + \left(\frac{\partial \Phi_{i,j}^{kl}}{\partial Z_{\text{wet},i}}\right) \delta Z_{\text{wet},i} \tag{4}$$

where $m_{\text{dry}}(E_i^k)$ and $m_{\text{wet}}(E_i^k)$ are mapping functions defined above, and $\left(\frac{\partial \Phi_{i,j}^{kl}}{\partial Z_{\text{wet},i}}\right) \delta Z_{\text{wet},i}$ is the time-varying effect due to the Z_{wet}; this correction is estimated using the chosen mapping function. A similar expression on the basis of $\delta Z_{\text{wet},i}$ and $\delta Z_{\text{wet},j}$ can be derived for $T(E_i^l)$, $T(E_j^k)$, and $T(E_j^l)$, respectively.

The Marini mapping function with the Marini tropospheric model

As mentioned above, among the comparison of three different mapping functions with their corresponding tropospheric models, Marini seems to be the best option according to preliminary results obtained with PAGES software. It is well known that the Marini model shows that the elevation angles of the tropospheric path delay could be expressed as a continued fraction in terms of the sine of the elevation angle E and is given by the so-called Marini mapping function, presented by (Marini 1972).

$$m_{wet}Mar(E) = \cfrac{1}{\sin(E) + \cfrac{a_{wet}}{\sin(E) + \cfrac{b_{wet}}{\sin(E) + \cfrac{c_{wet}}{\sin(E) + \ldots}}}} \tag{5}$$

with

$$\begin{aligned} a_{\text{wet}} &= 0.001185 + 0.6071 \times 10^{-4}(P_0 - 1000) \\ &\quad - 0.1471 \times 10^{-3} e_0 + 0.3072 \times 10^{-2}(T_0 - 20) \\ &\quad + 0.1965 \times 10^{-1}(\beta + 6.5) \\ &\quad - 0.5645 \times 10^{-2}(h_T - 11.231) \end{aligned}$$

$$\begin{aligned} b_{\text{wet}} &= 0.00114 \times (1 + 0.1164 \times 10^{-4}(P_0 - 1000) \\ &\quad + 0.2795 \times 10^{-3} e_0 + 0.3109 \times 10^{-2}(T_0 - 20) \\ &\quad + 0.3038 \times 10^{-1}(\beta + 6.5) \\ &\quad - 0.1217 \times 10^{-1}(h_T - 11.231)) \end{aligned}$$

$$c_{\text{wet}} = -0.0090$$

Several researchers have improved these constants with only small changes on the coefficients given on Eq. 5 (Chao 1973; Davis et al. 1985; Ifadis 2000); but, so far, all mapping functions are based on meteorological parameters. According to Troller (2004), the accuracy of all mapping functions is ±1 cm or better where the main difference is the elevation angle range for which this accuracy is valid.

Precipitable water vapor from GPS

The integrated amount of water vapor in the zenith direction is called precipitable water vapor (PWV). PWV is approximately proportional to the tropospheric path delay, which can be estimated from GPS measurements. GPS radio signals are delayed by the ionosphere and troposphere layers on their way from the satellite to the receiver antenna on the ground. The delay caused by the neutral atmosphere can be used to retrieve the PWV from the ground-based GPS observations collected at sites with known locations. In the approach to estimate PWV, the time-varying part of the Z_{wet}, which is coupled with the PWV above the GPS receiver, was estimated using the Marini mapping function, namely $m_{\text{wet}}\text{Mar}(E)$. On the other hand, the constant part was evaluated using the corresponding Marini tropospheric model, and it was subsequently transformed to PWV following the standard approach as proposed by Bevis et al. (1992),

$$\text{PWV}_{\text{GPS}} = (Z_{\text{wet}}) \frac{10^6}{w_{\text{den}} \cdot R_{wv}\left(\frac{k_3}{T_m} + k_2\right)} \tag{6}$$

where w_{den} is the density of liquid water, R_{wv} is the specific gas constant for water vapor, k_3 and k_2 are the refractivity constants, T_m is the weighted mean temperature of the atmosphere defined by Davis et al. (1985). According to Bevis et al. (1996), the significance of Eq. 6 lies in the fact that it allows for a transformation of the PWV estimate, derived from an operational numerical weather model, into an estimate of Z_{wet}. In order to perform these transformations, one must be able to form a prior estimate of the time-varying parameter on the right hand side of Eq. 6, which is a function of various local physical constants and the mean temperature T_m of the atmosphere. These values can be obtained from the vertical profiles as shown by Wang et al. (2005)

$$T_m \approx \frac{\sum_{i=1}^{N}\left(\frac{e_i}{T_i}\Delta p_i\right)}{\sum_{i=1}^{N}\left(\frac{e_i}{T_i^2}\Delta p_i\right)} \tag{7}$$

where e is the water vapor pressure, and T is the temperature. Equation 7 can also be expressed in terms of the observations of the height z instead of the pressure p. In this experiment, surface pressure was used, since the observations of p are readily available, and both are related to each other assuming a hydrostatic equilibrium, which is valid for Antarctica. However, in order to obtain the T_m value in Eq. 6, Bevis et al. (1994) developed the following linear relationship between T_m and the surface temperature T_s, which was derived from radiosonde data at 13 US sites over a 2-year period with an RMS error of $\sim$4.74 K,

$$T_m = a + bT_s \tag{8}$$

where a and b generally depend on the region. In Eq. 8, the coefficients a and b were generated by Bevis et al. (1994) specifically for the United States., giving $a = 70.2$ and $b = 0.72$. The PAGES software uses these coefficients in the procedure to obtain PWV from the Z_{wet}. However, these values might not be the appropriate ones for the Antarctic TAMDEF stations since the tropospheric conditions there are different from those experienced at GPS stations across the United States. For example, Liou and Teng (2001) and Liu et al. (2005) obtained values of $a = -31.5$ and $b = 1.07$ for Taipei, and $a = 44.5$ and $b = 0.81$ for the Tibetan Plateau. Nevertheless, Wang et al. (2005) provide a complete analysis of the relative error on GPS-PWV due to errors in T_m using Eq. 7, coming up with

$$\frac{\Delta \text{PWV}_{\text{GPS}}}{\text{PWV}_{\text{GPS}}} = \frac{1}{1+\frac{k_2}{k_3}T_m}\cdot\frac{\Delta T_m}{T_m} \approx \frac{\Delta T_m}{T_m} \tag{9}$$

considering the fact that the relation between k_2/k_3 is small ($\approx 5.9 \times 10^{-5} K^{-1}$).

On the basis of Eq. 9, Wang et al. (2005) shows that for T_m ranging from 240 to 300 K, the 1 and 2% accuracies in GPS-PWV require errors in $T_m < 2.74$ K and 5.48 K on average, respectively. Hence, the relative error of GPS-PWV approximately equals to that of T_m Finally, Bevis et al. (1994) indicate that in order to obtain T_m rigorously, the vertical profile of temperature and water vapor pressure is needed, plus accurate and simultaneous surface pressure and temperature measurements at the site locations for accurate estimates of GPS-PWV.

Numerical weather prediction water vapor

Since the GPS-PWV estimates are able to reproduce the variability seen in the radiosonde measurements, the GPS values can thus be compared with PWV values extracted from the AMPS, which is a mesoscale numerical weather prediction model that has been tuned to work in the Antarctic environment and provides guidance for operations-based forecasts for the US Antarctic Program. Bromwich et al. (2005) have demonstrated that the moisture prediction capability of AMPS is the lowest of the model field; thus, comparing the AMPS forecasts with the GPS-PWV estimates will allow for a better understanding of the model's prediction of moist processes. In the future, it is expected that assimilated TAMDEF GPS-PWV estimates will aid in improving the moisture prediction in AMPS, thereby leading to increased forecast accuracy, which is essential for any extended research operations conducted across the Antarctic continent. However, observations of the moisture in the atmosphere in and around the McMurdo region are very limited; thus, it is very difficult to quantify the performance of the model in this important area. One set of available moisture observations, namely in the form of PWV derived from stationary GPS recorders, offers a unique data set that covers a geographically and meteorologically diverse area of the McMurdo region. The use of GPS-derived PWV is becoming more common in validating numerical weather forecasts (Vey et al. 2004; Liu et al. 2005; Vey and Dietrich 2008). As such, there is significant potential to substantially extend the understanding of the McMurdo region in this collaborative effort between the USAP atmospheric and geological science initiatives. PWV is evaluated with AMPS by using the following

$$\text{PWV}_{\text{AMPS}} = \frac{1}{g}\int_{p\_\text{sfc}}^{p\_\text{top}} q\,\mathrm{d}p \tag{10}$$

where g is the gravitational constant ($\sim$9.81 ms^{-2}), $p_$sfc is the atmospheric pressure at the surface, $p_$top is the atmospheric pressure at the top of the atmosphere, and q is the specific humidity. The specific humidity is the mass of the dry air (the atmosphere minus water vapor), divided by

the total mass of atmosphere. It is usually expressed in g/kg. AMPS and calculates the specific humidity, which is related to relative humidity, dew point temperatures, and other moisture indices, and then integrates this throughout the atmospheric column to calculate the PWV.

Water vapor radiosonde

To determine the quality of GPS-derived PWV, the estimates for MCM4 are compared to the McMurdo radiosonde measurements of PWV. Radiosondes are weather-balloon-launched instrument packages that measure upper air profiles of temperature, pressure, and humidity of the atmosphere. Also, wind speed and direction can be measured by monitoring the balloon's progress from ground level to altitudes in excess of 30 km. Radioactivity and ozone measurements can also be obtained using this technique. The observed data are transmitted to the equipment located on the ground in order to be processed into weather messages. The Space Science and Engineering Center (SSEC), University of Wisconsin-Madison (UW-Madison), generated the water vapor radiosonde daily solutions with a 12-h interval, for only one of the TAMDEF/IGS sites analyzed in this experiment. Strictly speaking, MCM4 was the only site where both the water vapor radiosonde and the PWV from GPS were compared, due to the fact that radiosonde data for the rest of the TAMDEF stations are not available. The algorithm used to estimate the water vapor from radiosonde data is described in the following. Usually, by using radiosonde profiles, it is possible to calculate the total amount of water vapor by integrating the measurements as

$$\mathrm{PWV}_{\mathrm{Radson}} = \int \rho_{wv}(z)\mathrm{d}z \tag{11}$$

where ρ_{wv} is the water vapor mass density at altitude z. The value ρ_{wv} can be obtained from the relative humidity RH and the measured temperature T as

$$\rho_{wv} = \mathrm{RH} \cdot e_s \cdot \frac{1}{R_{wv} \cdot T} \tag{12}$$

where e_s is the saturation water vapor pressure that depends on temperature, and R_{wv} is the specific gas constant for water vapor. Traditionally, if the water vapor is directly measured by radiosondes, the wet zenith delay can be derived from it by means of Eq. 11. The radiosondes measure the wet zenith delay with high-quality vertical resolution but poor horizontal resolution and varying temporal resolution. Since most of the residual tropospheric delays result from the tropospheric wet component, radiosondes provide a good way to measure the residual tropospheric delay. However, these devices are relatively expensive and only limited measurements are available; usually two launches per day during the summer field season and one launch per day during the polar winter at MCM4.

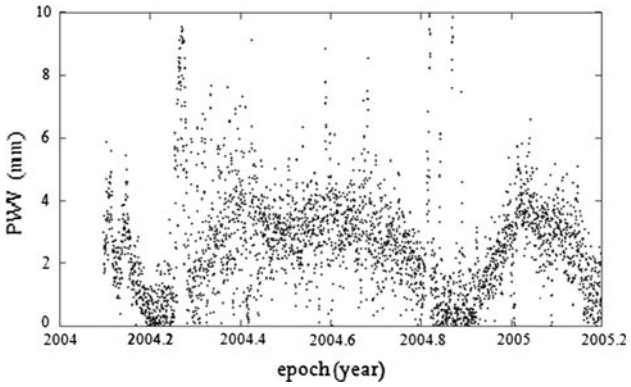

Fig. 9 GPS-PWV time series at FIE0

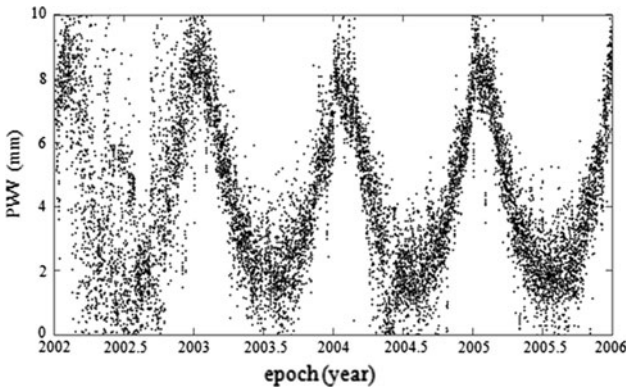

Fig. 10 GPS-PWV time series at MCM4

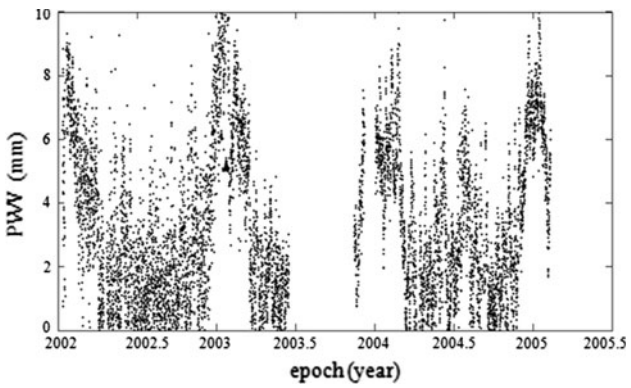

Fig. 11 GPS-PWV time series at ROB1

Results and analysis

Figures 9, 10, 11 illustrate the GPS-PWV time series, computed for each of the three TAMDEF sites using the

Table 2 GPS-PWV statistics

Site	M. function and tropo model	Max (mm)	Mean (mm)	SD ±(mm)
FIE0	Marini	9.9	2.4	1.6
MCM4	Marini	10.8	4.2	2.6
ROB1	Marini	9.9	3.4	2.3

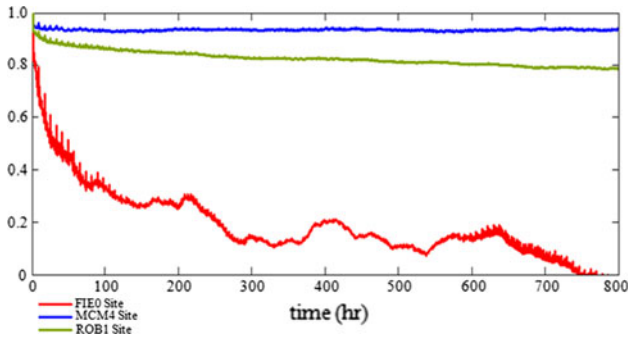

Fig. 12 Auto-covariance at FIE0, MCM4 and ROB1

Marini mapping function. The GPS-PWV ranges from 0 to 10 mm for FIE0 and ROB1 and from 0 to 11 mm for the MCM4 site. A clear seasonal effect can be observed in the graph for MCM4, with more noise in PWV for 2002. This fact could be attributed to the hardware change when the AOA SNR-12 ACT replaced the ROGUE SNR-8000 GPS receiver on January 3, 2002. The values for the PWV are higher in summer and lower in winter due to the greater moisture storing capacity of the warmer summer atmosphere. The FIE0 and ROB1 PWV estimates look nosier in comparison with MCM4, and the seasonal effect is barely seen. Recall that FIE0 site is located in a more marine-influenced atmospheric environment; thus, the GPS-PWV estimates might be more sensitive to possible changes when using the corresponding Marini mapping function, resulting in more disperse results. However, the reason for more noise in these data is not fully understood and this issue requires more investigation. In addition, the maximum, mean, and standard deviations of the GPS-PWV results for each of the three sites are presented in Table 2. Here, it can be shown for the TAMDEF sites that GPS can provide estimates of PWV with an accuracy of ±2.6 mm. The largest difference in mean is 1.8 mm between FIE0 and MCM4, and the smallest difference is 0.8 mm between MCM4 and ROB1.

Figure 12 shows the auto-covariance for GPS-PWV values computed for each of the three tested sites. It can be observed that the signal does not decorrelate for the MCM4 and ROB1 sites; however, there is a drop off of the signal for FIE0, which is more influenced by its marine environment that might be causing more noisy results. Further investigation may be required if surface meteorological data become available in the future.

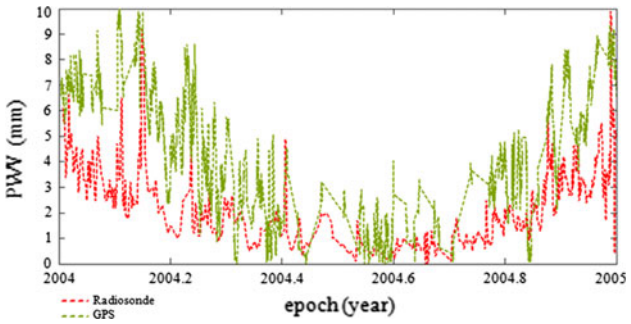

Fig. 13 GPS-PWV estimated every 3 h versus radiosonde PWV values estimated every 12 h at MCM4

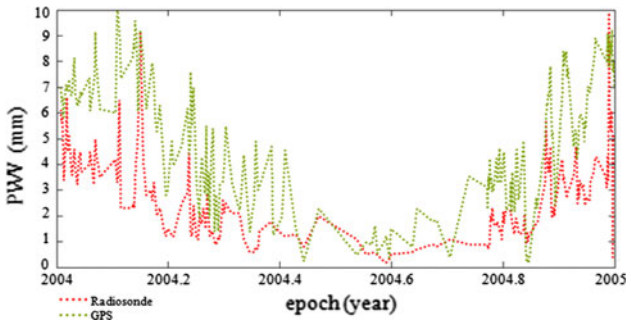

Fig. 14 One-to-one comparison of GPS-PWV versus radiosonde PWV values at MCM4

Table 3 Statistics of the one-to-one comparison of GPS-PWV versus radiosonde PWV at MCM4

Site	PWV from	Max (mm)	Mean (mm)	SD ±(mm)
MCM4	Radiosonde	9.9	2.7	1.6
MCM4	GPS	9.9	4.9	2.4

Figure 13 illustrates the comparison between estimates of GPS-PWV using external meteorological information, such as surface temperature and pressure, with radiosonde PWV data at the MCM4 site for the year 2004. It can be observed that GPS-PWV estimated every 3 h consistently exceeds the radiosonde PWV values estimated every 12 h. Therefore, Fig. 14 shows the one-to-one comparison between the GPS-PWV and radiosonde PWV at the same MCM4 site that shows more coincidence than the previous comparison.

Table 3 illustrates the statistics for the one-to-one comparison of GPS-PWV versus radiosonde PWV values at MCM4, both estimated every 12 h. The difference in the mean value between radiosonde PWV and GPS-PWV is of 2.2 mm. Hence, in order to more closely investigate about

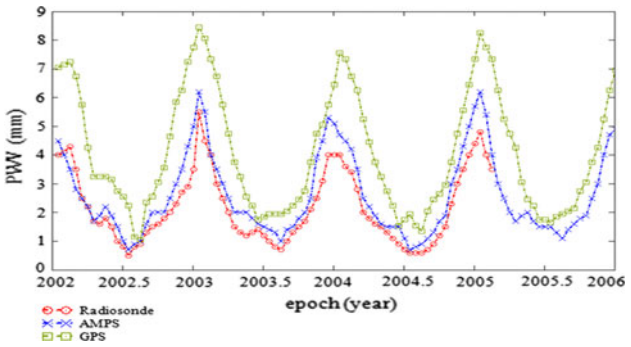

Fig. 15 Monthly mean PWV comparisons at MCM4

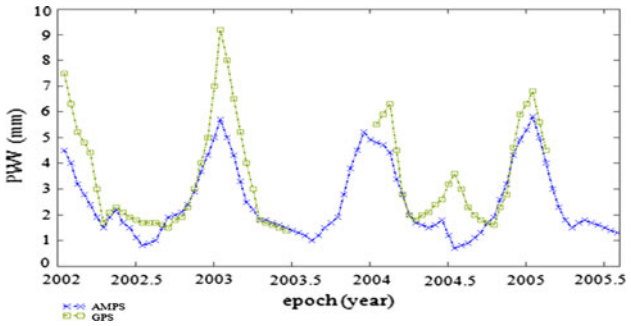

Fig. 16 Monthly mean comparison at ROB1 site

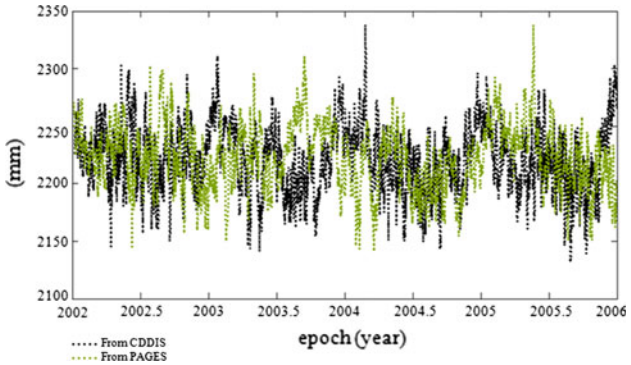

Fig. 17 Total wet zenith delay at MCM4 estimated by PAGES and CDDIS

Table 4 GPS-PWV statistics at MCM4

MCM4 site	Mean (mm)	SD ±(mm)
GPS-PWV	3.9	1.9
AMPS-PWV	2.6	1.4
Radiosonde PWV	2.2	1.3

Table 5 Biases in PWV by season at MCM4 differencing AMPS and GPS

Biases	DJF	MAM	JJA	SON	Annual
2002	−4.32	−1.91	−0.89	−0.98	−3.47
2003	−1.06	−0.59	−0.32	−0.35	−1.67
2004	−0.50	−0.34	−0.21	−0.25	−1.08
2005	−0.36	*	*	*	−0.20
Overall	−1.96	−0.95	−0.47	−0.53	−2.07

mean differences at the MCM4 site, the monthly mean comparisons between the radiosonde PWV, AMPS-PWV, and GPS-PWV values are shown in Fig. 15. The seasonal effect addressed before for GPS-PWV estimates can clearly be seen in the plotted results. A close agreement between radiosonde PWV and AMPS-PWV mean values is observed as well, with differences of 0.4 mm. The presence of a consistent positive bias of 1.7 mm of GPS-PWV with respect to radiosonde and a 1.3 mm with respect to AMPS-PWV is also revealed. The reason for the bias, however, must still be determined. A potential contributor to this bias could be the antenna phase center variation at the MCM4 site, which has not been calibrated, as mentioned above. Note that the antenna phase center miscalibration or the lack of proper calibration parameters will directly have an impact on the GPS-PWV estimates (Table 4).

In addition, the biases were analyzed by season, following the proposed classification: *Annual* = average for the whole year of mean value for AMPS minus mean value for GPS-PWV; *DJF* = December–January–February average (austral summer); *MAM* = March–April–May average (austral fall); *JJA* = June–July–August average (austral winter); and *SON* = September–October–November average (austral spring).

The results from the above classification are shown in Table 5, with the smallest values of the bias occurring during the winter and the highest values during the summer. Overall, the year 2002 shows the biggest biases ranging from −0.89 to −4.32. The symbol * indicates that no PWV data were available to compare them with GPS-PWV.

Figure 16 presents a plot of the monthly means from the ROB1 station situated northeast of MCM4 and located in a marine environment. A better alignment can be observed, as compared to MCM4, with the mean bias of −0.79 mm larger in summer as compared to other seasons. Here, the PAGES software was used, but considering only annual means for external surface temperature and surface pressure. These results require special attention and further investigation.

Summarizing, the GPS-PWV estimates for the MCM4 site were compared to the radiosonde and the AMPS-PWV. This comparison revealed a consistent positive bias of 1.7 mm with respect to radiosonde and a 1.3 mm with respect to AMPS. A potential contributor to this bias could

Table 6 Statistics of the Total Wet Zenith Delay at MCM4

TWZD from	Max (mm)	Min (mm)	Mean (mm)	SD ±(mm)
CDDIS	2,338.4	2,131.4	2,221.8	27.97
PAGES	2,338.7	2,141.0	2,222.9	27.57
CDDIS—PAGES	−0.3	−9.6	−1.07	0.40

be the antenna phase center variation at the MCM4 site, which has not been calibrated. Note that the antenna phase center miscalibration will directly impact the PWV estimates. Another potential contributor could be the PAGES software that uses specific values for the coefficients of the linear regression between surface temperature and T_m in the procedure to estimate water vapor from the wet zenith delay. These coefficients were derived exclusively under US conditions. These values might not be appropriate for the Antarctic TAMDEF stations since the tropospheric conditions there are different from those experienced by GPS stations across the United States. Furthermore, in order to validate the total wet zenith delay (TWZD) estimates at the MCM4 site using PAGES software, these estimates were directly compared to the TWZD computed every 3-h by the CDDIS analysis center as shown in Fig. 17. Some statistics for both solutions are presented in Table 6. The results are very comparable with 1.1 mm difference in the mean value and ±0.4 mm in this standard deviation. Also, the range from both solutions looks similar, with only <1% difference with respect to the minimum value; thus, the reason of the small positive bias in the GPS-PWV should come from another source.

Conclusions and recommendations

A GPS-PWV estimation analysis was presented for three Antarctic sites, FIE0, MCM4, and ROB1, using double-difference ionosphere-free observations with fixed ambiguities, and the Marini mapping function with the corresponding Marini tropospheric model. The GPS-PWV estimates for the MCM4 site were compared with the radiosonde PWV data and AMPS-PWV. This comparison revealed a consistent bias of 1.7 mm between the GPS solution and the radiosonde reference values. However, GPS observations can provide a unique set of moisture data, a field that is challenging to accurate forecasting, especially in areas such as Antarctica where weather station coverage may not be sufficient. In general, GPS data are at higher temporal and spatial resolutions than any available meteorological data. It should also be mentioned that GPS-based PWV estimation and data availability are quite established in midlatitudes, while more investigation is still needed at higher latitudes. The presented PWV results in the Antarctic environment are encouraging, further research continues. However, it is too early to discern yet if GPS-PWV results in Antarctic environment would provide sufficient accuracy to justify the assimilation into the AMPS system. More testing and algorithmic tuning is needed for the methodology of extracting the PWV values. Employing coefficients specific to Antarctica in the relationship given by Eq. 8 will likely help to reduce the bias. Quality control, data filtering, and site-specific corrections need to be conducted on the GPS data to tune the measurements, which should improve the correlation between GPS-PWV and AMPS-PWV and lower the overall bias in the GPS-PWV. The uncalibrated antenna at MCM4 remains a problem.

Acknowledgments The authors would like to thank Dr. Matthew A. Lazzara and Shelley L. Knuth from the Space Science and Engineering Center, University of Wisconsin-Madison, for providing the radiosonde PWV data series for McMurdo. Thanks to Dr. Mark Schenewerk for his valuable comments on dealing with troposphere in PAGES. Special thanks go to Dr. Terry Wilson and Mike Willis from the School of Earth Sciences at OSU and the United States Geological Survey Antarctic Mapping group for providing the TAMDEF data. This research was supported by a National Science Foundation grant.

References

Bevis M, Businger S, Herring TA, Rocken C, Anthes RA, Ware RH (1992) GPS meteorology: remote sensing of atmospheric water vapor using the global positioning system. J Geophys Res 97:l5787–l15801

Bevis M, Businger S, Chiswell SR, Herring TA, Anthes RA, Rocken C, Ware RH (1994) GPS meteorology: mapping zenith wet delay onto precipitable water. J Appl Meteorol 33:379–386

Bevis M, Chiswell S, Businger S (1996) Estimating wet delays using numerical weather analyses and predictions. Radio Sci 31(3):477–487

Bromwich DH, Fogt RL (2004) Strong trends in the skill of the ERA-40 and NCEP/NCAR reanalyses in the high and middle latitudes of the Southern Hemisphere, 1958–2001. J Clim 17:4603–4619

Bromwich DH, Monaghan AJ, Powers JG, Manning KW (2005) Real-time forecasting for the Antarctic: an evaluation of the Antarctic Mesoscale Prediction System (AMPS). Mon Weather Rev 133:579–603

Chao C (1973) A model for tropospheric calibration from daily surface and radiosonde balloon measurement. Technical Memorandum, pp 391–350. Jet Propulsion Laboratory, Pasadena California

Davis JL, Herring TA, Shapiro I, Rogers AE, Elgered G (1985) Geodesy by radio interferometry: effects of atmospheric modeling errors on estimates of baseline length. Radio Sci 20(6):1593–1607

Dodson AH, Shardlow PJ, Hubbard LCM, Elegered G, Jarlemark POJ (1996) Wet Tropospheric effects on precise relative GPS height determination. J Geod 70(4):188–202

Eckl MC, Snay RA, Soler TA, Cline MW, Mader GL (2001) Accuracy of GPS-derived relative positions as a function of interstation distance and observation-session duration. J Geod 75:633–640

Emardson TR, Simons M, Webb FH (2003) Neutral atmospheric delay in interferometric synthetic aperture radar applications: statistical description and mitigation. J Geophys Res 108(B5): 2231. doi:10.1029/2002JB001781

Fogt RL, Bromwich DH (2008) Atmospheric moisture and cloud cover characteristics forecast by AMPS. Weather Forecast 23:914–930

Ifadis IM (2000) A new approach to mapping the atmospheric effect for GPS observations. Earth Planets Space 52:703–708

Lancaster P, Salkauskas K (1986) Curve and surface fitting: an introduction. Academic Press, Harcourt Brace Jovanovich, New York

Liou YA, Teng YT (2001) Comparison of precipitable water observations in the near tropics by GPS, microwave radiometer, and radiosondes. J Appl Meteorol 40:5–15

Liu J, Sun Z, Liang H, Xu X, Wu P (2005) Precipitable water vapor on the Tibetan Plateau estimated by GPS, water vapor radiometer, radiosonde, and numerical weather prediction analysis and its impact on the radiation budget. J Geophys Res 110:D17106

Mader GL, Schenewerk MS, Ray JR, Kass WG, Spofford PR, Dulaney RL, Pursell DG (1995) GPS orbit and earth orientation parameter production at NOAA for the International GPS service for geodynamics for 1994. In: Zumberge JF et al (eds) International GPS service/or geodynamics 1994 annual report. California Institute of Technology, Pasadena, CA, Jet Propulsion Lab, pp 197–212

Marini JW (1972) Correction of satellite tracking data for an arbitrary tropospheric profile. Radio Sci 7(2):223–231

Marshall J, Schenewerk M, Snay R (2001) The effect of the MAPS weather model on GPS-determined ellipsoidal heights. GPS Solut 5(1):1–14

Powers JG, Monaghan AJ, Cayette AM, Bromwich DH, Kuo Y-H, Manning KW (2003) Real-time mesoscale modeling over Antarctica: the Antarctic Mesoscale Prediction System (AMPS). Bull Am Meteor Soc 84:1533–1545

Schenewerk M (2004) Workshop in PAGES. The Ohio State University, Columbus OH

Schenewerk MS, Marshall J, Dillinger W (2001) Vertical ocean loading deformations derived from a global GPS network. J Geod Soc Jpn 47(1):237–242

Troller M (2004) GPS-based determination of the integrated and spatially distributed water vapor in the troposphere. Geodätisch-geophysikalische Arbeiten in der Schweiz, vol 67. Swiss Geodetic Commission

Vázquez GE (2009) Geodesy in Antarctica: a pilot study based on the TAMDEF GPS network, Victoria Land, Antarctica. PhD Thesis, Geodetic Science Department, The Ohio State University, Columbus, OH

Vázquez GE, Brzezinska D (2005) Precipitable water vapor from GPS in Antarctica: opportunities from the TAMDEF GPS network, Victoria Land. Poster at the AGU Fall Meeting. San Francisco CA

Vey S, Dietrich R (2008) Validation of the atmospheric water vapour content from NCEP using GPS observations over Antarctica. In: Capra A, Dietrich R (eds) Geodetic and geophysical observations in Antarctica–an overview in the IPY perspective. Springer, Berlin, pp 125–136

Vey S, Dietrich R, Johnsen K-P, Miao J, Heygster G (2004) Comparison of tropospheric water vapour over Antarctica derived from AMSU-data, ground-based GPS data and the NCEP/NCAR reanalysis. J Meteorol Soc Jpn 82:259–267

Wang J, Zhang L, Dai A (2005) Global estimates of water-vapor-weighted mean temperature of the atmosphere for GPS applications. J Geophys Res 110:D21101

Author Biographies

Vázquez B. G. Esteban is an assistant professor at the Autonomous University of Sinaloa, Mexico. His research interest covers GPS atmospheric research and precise DGPS static positioning and deformations. He is currently a member AGU, IAG and ION and recipient of the 2006 ION Graduate Student Award.

Dorota A. Grejner-Brzezinska is a Professor and leader of the SPIN Laboratory at The Ohio State University. Her research interests covers GPS kinematic positioning, precise orbit determination of GPS/LEO, INS/GPS/image/LiDAR integration. She is the 2005 recipient of the USGIF Research Award and the ION Thurlow Award. She is a Fellow of the IAG.